UNCLASSIFIED DTIC FILE COPY

SECURITY CLASSIFICATION OF THIS PAGE

(2)

REPORT DOCUMENTATION PAGE

1a. REPORT SECURITY CLASSIFICATION: Unclassified	1b. RESTRICTIVE MARKINGS
2a. SECURITY CLASSIFICATION AUTHORITY	3. DISTRIBUTION/AVAILABILITY OF REPORT: Approved for public release, distribution unlimited
2b. DECLASSIFICATION/DOWNGRADING SCHEDULE	
4. PERFORMING ORGANIZATION REPORT NUMBER(S)	5. MONITORING ORGANIZATION REPORT NUMBER(S): AFOSR-TR- 89-0331
6a. NAME OF PERFORMING ORGANIZATION: NASA/Jet Propulsion Laboratory	6b. OFFICE SYMBOL (If applicable): JPL
6c. ADDRESS (City, State and ZIP Code): 4800 Oak Grove Drive, M/S 125/224, Pasadena, CA 91109	7a. NAME OF MONITORING ORGANIZATION: Air Force Office of Scientific Research
	7b. ADDRESS (City, State and ZIP Code): AFOSR/NA, Bolling AFB, DC 20332-6448
8a. NAME OF FUNDING/SPONSORING ORGANIZATION: AFOSR	8b. OFFICE SYMBOL (If applicable): NH
8c. ADDRESS (City, State and ZIP Code): Same as 7b.	9. PROCUREMENT INSTRUMENT IDENTIFICATION NUMBER: AFOSR-ISSA-87-00446
	10. SOURCE OF FUNDING NOS.

PROGRAM ELEMENT NO.	PROJECT NO.	TASK NO.	WORK UNIT NO.
61102F	2308	A1	

11. TITLE (Include Security Classification): MPD Thruster Erosion Research (u)

12. PERSONAL AUTHOR(S): King, David Q., Callas, John L.

13a. TYPE OF REPORT	13b. TIME COVERED	14. DATE OF REPORT (Yr., Mo., Day)	15. PAGE COUNT
Final	FROM 1/1/87 TO 12/31/87	88 11 30	33

16. SUPPLEMENTARY NOTATION

17. COSATI CODES			18. SUBJECT TERMS (Continue on reverse if necessary and identify by block number)
FIELD	GROUP	SUB. GR.	Electric Propulsion Magnetoplasma Dynamic Thruster, Cathode Lifetime
346			

19. ABSTRACT (Continue on reverse if necessary and identify by block number)

Research covering 3 aspects of MPD thruster physics is discussed: First, a significant operational problem which has limited the useful operation of the device is discussed. This is severe erosion of the insulator at the cathode insulator junction. A technique which appears to solve the problem has been tested, and is described. Second, a preliminary analyses of anode sheath is presented. Third, and lastly, analysis of the discharges two dimensional nature is explored with for the case where transverse gradients are considered but transverse velocity is assumed to be zero. This situation applies to high aspect ratio devices. The analyses concludes with: a) a formalism that provides a means to qualitatively evaluate Ohmic dissipation from simple measurements of magnetic field; b) discussion of the Hall effect on gas dynamic choking; and c) discussion of the Hall effect on magnetosonic choking (where thermodynamics is ignored).

20. DISTRIBUTION/AVAILABILITY OF ABSTRACT	21. ABSTRACT SECURITY CLASSIFICATION
UNCLASSIFIED/UNLIMITED ☒ SAME AS RPT. ☒ DTIC USERS ☒	(u)

22a. NAME OF RESPONSIBLE INDIVIDUAL	22b. TELEPHONE NUMBER (Include Area Code)	22c. OFFICE SYMBOL
[redacted] Dr. Robert A. Brown	[redacted] (202) 767-4938	NH

DD FORM 1473, 83 APR — EDITION OF 1 JAN 73 IS OBSOLETE

UNCLASSIFIED
SECURITY CLASSIFICATION OF THIS PAGE

Contract NAS7-918
Task Order RE-182, Amendment 292
Report Number: JPL D-6020

MPD THRUSTER EROSION RESEARCH

Annual Report
For the Period January-December 1987

By

David Q. King, Principle Investigator
and John L. Callas, Co-Investigator

Electric Propulsion and
Plasma Technology Group

JET PROPULSION LABORATORY
California Institute of Technology
Pasadena, California

November, 1988

Prepared for

Air Force Office of Scientific Research
AFOSR/NA
Bolling AFB
D.C. 20332

Table Of Contents

ABSTRACT 4

NOMENCLATURE 4

INTRODUCTION 5

SCIENTIFIC OBJECTIVES FOR FY87 5

STATUS 6
- INSULATOR/CATHODE INTERFACE 7
- ANODE SHEATH PRELIMINARY ANALYSIS 8
- QUASI 1-D THEORY 13

SUMMARY 23

REFERENCES 33

List of Tables and Figures

Table 1: Input Parameters to PLASMA.FOR 11
Figure 1 - 100 kW MPD Test Bed Schematic 25
Figure 2 - Detail of Insulator Erosion 26
Figure 3 - Buffer Electrode Schematic 27
Figure 4 - Self-Field Steady-State MPD Thruster Operating at 23 kW, 0.16 g/s Argon, 1200 A, for a 83 minute run 28
Figure 5 - Anode Sheath Electric Field vs Distance from Anode 29
Figure 6 - Plasma Potential vs. Distance from Anode 30
Figure 7 - Charge Density vs. Distance from Anode 31
Figure 8 - Ohmic Dissipation vs. Distance from Anode 32

ABSTRACT

Research covering three aspects of MPD thruster physics is discussed: First, a significant operational problem which has limited the useful operation of the device is discussed. This is severe erosion of the insulator at the cathode insulator junction. A technique which appears to solve the problem has been tested, and is described. Second, a preliminary analyses of the anode sheath is presented. Third, and lastly, analysis of the discharges two dimensional nature is explored with for the case where transverse gradients are considered but transverse velocity is assumed to be zero. This situation applies to high aspect ratio devices. The analyses concludes with: a) a formalism that provides a means to qualitatively evaluate Ohmic dissipation from simple measurements of magnetic field, b) discussion of the Hall effect on gas dynamic choking, and c) discussion of the Hall effect on magnetosonic choking (where thermodynamics is ignored).

NOMENCLATURE

- ρ Density (kg/m^3)
- β Hall Parameter
- σ Conductivity (σ_e denotes scalar conductivity)
- A Transverse Channel Dimension (m)
- $\underline{B}$ Magnetic Field Vector
- e Unit of Charge (+1.6021E-19 Coulomb)
- $\underline{E}$ Electric Field Vector (V/m)
- G Equation of State
- h Enthalpy (J/kg)
- $\underline{J}$ Current Density (A/m^2)
- $\dot{m}$ Propellant Mass Flow (kg/s)
- m Electron Mass
- n Number Density (m^{-3})
- P Pressure (Pa)
- s Ion Slip Parameter
- $\underline{u}$ Velocity vector (m/s)

Subscripts

- e Electrons
- i Ions
- n Neutrals

INTRODUCTION

The multimegawatt MPD thruster is an electric engine capable of orbital transfer and maneuvering of large payloads driven by a megawatt class space power supply. The MPD thruster is capable of specific impulses from 1,500 to 8,000 S, as demonstrated by thrust stand measurements at Princeton University. The high specific impulse means this electric system can perform missions using much less propellant than chemical systems. A five MW MPD electric system, propellant and payload from one shuttle launch must be replaced by the equivalent of four fully loaded Centaur G' stages. Thus, the savings in propellant and launch costs are very substantial.

The MPD thruster has been studied in research laboratories since its discovery in 1964. Early steady-state testing was compromised by high vacuum tank pressures, which resulted in entrainment and acceleration of ambient gas. Later work in the 70's was concentrated in pulsed, multimegawatt, quasi-steady mode to circumvent the need for costly steady-state pumping systems. In the quasi-steady mode, current is applied in a rectangular pulse much longer than plasma transients. This approach has permitted a variety of diagnostics to be applied in university research program. These show that efficiencies of 38% at 4,000 s are achievable with a primitive thruster design. Theory suggests that ultimately 50-60% is possible.

Presently, thruster research is focused on determining the lifetime of components. Principle is the cathode, which must operate under severe conditions while supplying some 20,000 amperes at 200-400 A/sqcm. Secondly, the anode must be studied to minimized losses in the anode sheath region, which may be as much as 10-20% of the total input power. Finally, the insulator must be studied to assess the role of plasma dynamic choking which governs the power input to the thruster.

SCIENTIFIC OBJECTIVES FOR FY87

The ultimate goal is to develop a multimegawatt MPD thruster with a lifetime of at least 1,000 hours and a thrust efficiency over 50%. To support this goal, component level studies must be conducted in realistic conditions. Physical issues key to the larger goal are:

1 Cathode physics with adjacent, high speed plasma flows

a. What is the effect of high speed and energy ions on the heat balance and electron emission processes?

b. Does the viscous boundary layer on the cathode preclude the high speed ions from bombarding and sputtering the cathode?

c. How do gas species, such as Neon, Nitrogen, and Argon affect the cathode physics?

2 Anode sheath physics

a. How is the anode fall voltage quantitatively related to the self-magnetic field strength?

b. Can the anode fall voltage be substantially modified by the addition of a solenoidal shaped field?

c. Does the anode sheath play a role in cathode erosion?

3 Choked Flow and Thermodynamics

a. Can the insulator shape be modified to affect the applied electric field at the axial halfway position, where the back EMF reaches it's peak?

b. Can spectroscopic studies of the temperature and plasma velocity be made in the arc discharge to prove the role of thermodynamics in thruster behavior?

STATUS

In pursuit of the above objectives, which were always considered beyond the scope of a single years effort, three major areas are reported. These cover (1) experimental status by

discussing the insulator-cathode interface, (2) a quasi one dimensional analysis pertinent to choked flow and thermodynamic issues, and (3) precursor analyses of the anode sheath region.

INSULATOR/CATHODE INTERFACE

DESCRIPTION OF PROBLEM: Severe erosion of the insulator at the cathode interface occurred in the newly designed, 100 kW MPD test bed, shown in figure 1. Figure 2 is a detail of the cathode insulator region showing the eroded part. Erosion occurred independent of the mass flow through the 0.25 mm annulus and independent of the presence or absence of the annulus. Schrade has reported erosion in this location in devices at U. Stuttgart, although the electrode configuration differs and the piece adjacent to the cathode is a floating potential, water cooled copper part. This erosion only occurs in U. Stuttgart devices during start up transients.

Japanese researchers have had severe erosion of cathodes at this interface, rather than the insulator, in pulsed, multimegawatt, quasi-steady devices. The problem was solved by adding a buffer electrode, essentially a tungsten tube inserted in the insulator and electrically isolated from the cathode.

Here two hypothesis regarding insulator erosion are considered:

Sheath Effects: Figure 3 shows a buffer electrode, insulator, cathode, and hypothetical sheath regions. By supposing the cold mass injected here results in low electron temperature and density, the sheath thickness of a few Debye lengths may be as much as 0.125-0.25 mm. If such regions exist, they permit the electrodes to impose zero axial electric field across the Debye space. In turn, zero axial electric field should preclude axial current conduction. The net theory: perhaps this arrangement prevents the arc from moving upstream and undermining the buffer electrode and insulator.

Retrograde Arc Motion: Discussions of this problem with Schrade related his theory of microarc spot motion to undermining of the insulator. Microarcs within the cathode sheath region curve upstream, and may bend over and touch down again on the cathode. The original spot may extinguish some nanoseconds later, leaving a new spot, micrometers upstream. The process manifests itself on a macroscopic scale as retrograde motion of the current attach-

ment. Further Schrade estimates that an axial pressure gradient of 20 Torr across this region should be enough to arrest the retrograde arc motion.

Experimental Results: Tests with a buffer electrode showed that non erosive operation could be achieved with a buffer electrode radial clearance of 0.18 to 0.30 mm. With smaller clearance, the buffer electrode would short out to the cathode, probably due to uneven thermal expansion. Both the cathode and buffer electrode expand in diameter an amount similar to the radial clearance of 0.18 mm, in heating from room temperature to 2000 C. With radial clearance above 0.30 mm, the current appeared to undermine and erode the buffer electrode. Figure 4 shows the 100 kW subscale device operating at a steady state, during a 1 hour 23 minute run where no damage occured to the insulator, cathode, or buffer electrode. The tip cathode temperature was approximately 1875-1950 C for the duration of the run. The anode lip temperature was approximately 1600 C, and varied strongly with temperature. Test have not been conducted to evaluate the two hypotheses at this time.

ANODE SHEATH PRELIMINARY ANALYSIS

STATEMENT OF PROBLEM: A significant anode [sheath] fall voltage is observed during the operation of MPD devices. This fall voltage, depending on operating conditions, can be as much as 50% of the total voltage applied to the MPD device. This results in an inefficiency (power loss) of an equivalent amount (up to 50%). This power loss ultimately results in substantial anode heating.

The anode sheath can be characterized as the boundary phenomenon established by an anode (an electron collector) in the presence of a plasma where a potential difference between the anode and the plasma exists. In the MPD the situation is much more complicated. First, the plasma exists in the presence of a magnetic field. Components of the plasma (i.e. electrons) may exhibit magnetized behavior (where the cyclotron frequency is greater than the collision rate). Second, the plasma must transport a large current density resulting in ohmic and Lorentz contributions to the dynamics. Source and sink phenomenon (ionization and recombination) exist. Additionally, there exists significant spacial and temporal variation of parameters which will complicate any simple attempts at modelling the anode sheath phenomenon.

The existence of an anode sheath or equivalently the presence of an electric field near the anode must manifest itself as the existence of a non-neutral charge density as specified by Gauss' law. Near the anode the assumption of charge neutrality therefore fails. In addition, the plasma may not be fully ionized. Therefore, three species of particles exist, electrons, ions and neutral atoms. This then further complicates the problem since the plasma now cannot be correctly treated as a single fluid.

OBJECTIVE: First, develop an understanding of the mechanism which contribute to the anode sheath. Second, develop a model incorporating these individual mechanisms. This model may first be formulated as a simplified analytical model. Ultimately, quantitative answers for a given MPD configuration (geometry and operating parameters) would be needed to assess MPD performance. Therefore, a computational-plasma-dynamic code incorporating the anode sheath mechanisms might be exploited. With the behavior of the anode sheath understood, steps may be taken in the laboratory (by possibly altering the MPD configuration and/or operating parameters) to minimize the detrimental impact the anode sheath has on MPD performance.

APPROACH: First, identify those mechanisms (e.g. pressure gradient, Lorentz force, plasma resistance, etc.) which contribute to the anode sheath (electric field). The dominant mechanisms may be identified by inspection of the complete set of magneto-hydrodynamic equations correctly expressed for the anode sheath environment. Assumptions relating to the appropriateness of the Navier-Stokes expressions for this environment will have to be justified. Other contributing mechanisms may be identified from experimental observations.

Second, assess the appropriateness of assumptions which may simplify the problem (e.g. 1-dimensional analysis, steady-state operation, isothermal plasma, etc.). Owing to the complicated nature of the anode sheath problem many assumptions are required to simplify the problem such that models may be developed for each of the mechanisms. Many assumptions can be made without loss of generality. However, some assumptions cannot be justified within the context of the problem.

Third, develop models for individual mechanisms (e.g. collisions, conductivity, ionization, etc.) drawing from existing techniques (e.g. Hall conductivity, Coulomb scattering, etc.). From the development of the models for the individual mechanisms within the anode sheath, the behavior of the sheath and corresponding fall voltage may to be revealed. Contributions

from highly simplified analytical models may provide useful insight into the behavior of the anode sheath.

Finally, a complete model of the anode sheath incorporating the individual mechanisms is sought with as few assumptions as possible. This may take the form of a computational-plasma-dynamic code where the equations of physics governing the MPD are transported through time and allowed to converge.

NARRATIVE OF EFFORTS: A baseline MPD device of known configuration and specified parameters was used to scope-out the contributions of each of the mechanisms in the anode sheath. This baseline MPD is based on experimental devices which have been run in the laboratory. The contribution estimates are used to support some of the modelling assumptions in terms of estimating what mechanisms may be dominant and which may be ignored.

A program called PLASMA was developed (in FORTRAN) to calculate characteristic parameters of a plasma in the presence of a magnetic field. The results from this program was used to scope-out the relative effects of the anode sheath mechanisms. The plasma characteristics and basic parameters as calculated by PLASMA for the baseline MPD plasma are shown in Table 1.

Electron Temperature [eV]	1.00 (0.116E+05 K)
Ion Temperature [eV]	0.50 (0.580E+04 K)
Electron Density [m^{-3}]	0.10E+21
Ion Density [m^{-3}]	0.10E+21
Ion Atomic Number	18.
Ion Atomic Weight	40.00
Magnetic Field [Tesla]	0.10
Plasma Frequency [Hz]	0.898E+11 (0.334E-02 m)
Debye Length [m]	0.743E-06
Electron Cyclotron Frequency [Hz]	0.280E+10 (0.107E+00 m)
Ion Cyclotron Frequency [Hz]	0.384E+05 (0.781E+04 m)
Electron Larmor Radius [m]	0.337E-04
Ion Larmor Radius [m]	0.644E-02
Electron Thermal Speed [m/s]	0.593E+06
Ion Thermal Speed [m/s]	0.155E+04
Beta	0.403E-02
Hall Parameter	0.879E+01
Mean Free Path [m]	0.340E-03
Collision Rate (e-i) [s^{-1}]	0.200E+10
Collision Rate (e-e) [s^{-1}]	0.500E+10
Collision Rate (i-i) [s^{-1}]	0.524E+08
Bremsstrahlung Frequency [Hz]	0.242E+15 (0.124E-05 m)
Bremsstrahlung Radiation [W/m^3]	0.162E+03
Synchrotron Radiation [W/m^3]	0.621E-01

Table 1: Input Parameters to PLASMA.FOR

After inspection of the Navier-Stokes equation for a steady-state plasma considering collisional effects, three dominant driving effects for the anode fall were isolated, ohmic losses across the anode sheath, back-EMF produced by the Lorentz force, and the electron pressure gradient across the anode sheath. These observations are consistent with generally accept theory.

Charge Density: Gauss' law specifies the resulting charge density produced by an electric field gradient. Observations of electric field gradients of order 10,000 volts/meter squared within the anode sheath with corresponding plasma densities of order 1.0E+20/cubic meter have been made in the laboratory. By Gauss' law this corresponds to a change in charge density of order 1.0E+12/cubic meter. This change is very small compared to the bulk plasma

density. This observation is different from a previous theories that the anode sheath would be very ion rarefied.

Generalized Conductivity (Ohmic and Back-EMF): This observation of approximate density uniformity across the anode sheath would indicate that the nature of the conductivity and the back-EMF are not significantly different from the bulk of the plasma if the plasma is assumed to be approximately isothermal. In fact, energy losses in the anode sheath possibly indicate hotter temperatures in the sheath which would mean higher conductivity (decreased ohmic and back-EMF effects). Additional, the Hall parameter would not appear to change significantly between the bulk plasma and the anode sheath. This would de-emphasize the influence of the magnetic field on the anode fall. Therefore, the strong electric field (plasma potential) observed in the anode sheath might be dominated by the charge density gradient.

Static-Case Electric Field: If ohmic and back-EMF effects are assumed to be small relative to charge density gradient effects, then a closed form analytic solution can be calculated for the electric field near the anode. The plasma was assumed to be static, with zero current and isothermal. The results of the solution for the electric field, plasma potential and charge density for the chosen baseline MPD are shown in Figures 5, 6, and 7. These results appear to be approximately consistent with observations from the laboratory.

Anode Heating: One component of the transport mechanism for the thermal load to the anode is identified to be the current electrons passing through the anode sheath potential, accelerating under the electric field and then being absorbed into the anode. These electrons experience many collisions in the sheath which in turn heats the region near the anode. This would indicate a non-isothermal plasma in the anode sheath region. Ionization effect may be significant in anode sheath. The ohmic power loss for the anode sheath region based of the static-case electric field solution above for the baseline MPD is shown in Figure 8.

Future Steps: The highlights mentioned above are preliminary and require additional investigation to improve on the theoretical assessments. Additionally, effects of neutral atoms, ionization and recombination has not been considered. Future studies will also include these considerations.

To fully understand the anode sheath and the MPD in general, a dynamic model incorporating the necessary mechanisms must be developed. Much work has been done on related Magneto-Hydrodynamic (MHD) codes. However, most work has been done only with electrical neutral plasmas. Currently an existing 2-dimension, non-ideal MHD code with cylindrical symmetry is being sought such that anode sheath phenomenon can be added and analyzed.

Ultimately, this research is intended to guide MPD experimentation in the laboratory with the aim of improving MPD thruster performance.

QUASI 1-D THEORY

The purpose of this analysis is to examine the role of the Hall parameter in the context of the simplest theoretical framework. Previous work by King, Lawless, and Subramaniam has exposed the effects of equilibrium, frozen, and non-equilibrium state relations on gas dynamic choking in a strict one dimensional channel. By allowing for transverse gradients with zero transverse velocity, the one dimensional analyses can be extended to include the rotation of the body force from the axial direction, while retaining reasonable mathematical simplicity.

Assumptions and Simplifications The analyses assumes:

* Long aspect ratio where field fringing at the ends is neglected
* Channel area (height) is slowly varying
* Zero transverse velocity
* Sheath voltages are constant with axial position (which is to say that sheath effects are ignored)
* Steady Flow
* Rate kinetics governed by statistical mechanics

* Continuum flow

* Viscosity is neglected

Governing Equations:

The equilibrium state equation is written in a convenient form:

$$P=\rho G(\rho,h) \tag{1}$$

Ohms Law (form as it appears in Mitchner and Kruger, Partially Ionized Gasses, John Wiley & sons, 1973):

$$\underline{E} + \underline{u} \times \underline{B} + \frac{\nabla p_e}{e n_e} = \frac{\underline{J} + \beta_e \underline{J} \times \underline{b} + s \underline{b} \times (\underline{J} \times \underline{b})}{\underline{\sigma}} \tag{2}$$

$$\underline{b} = \frac{\underline{B}}{|\underline{B}|} \qquad s = \left(\frac{\rho_n}{\rho}\right)^2 \beta_e \beta_i$$

$$\beta_e = \frac{\omega_e}{\nu_e} \qquad \beta_i = \frac{\omega_i}{\nu_i}$$

$$\underline{\sigma} = \begin{pmatrix} \sigma_\perp & -\sigma_\parallel & 0 \\ \sigma_\parallel & \sigma_\perp & 0 \\ 0 & 0 & \sigma_e \end{pmatrix} \qquad \sigma_\perp = \frac{\sigma_e}{1+\beta_e^2} \qquad \sigma_\parallel = \beta_e \sigma_\perp$$

Continuity equation:

$$\rho u_x A = \dot{m} \tag{3}$$

Y (transverse) momentum, assuming $u_y = 0$

$$0 = \frac{\partial}{\partial y}\left(P + \frac{B_z^2}{2\mu_0}\right)$$

OR

$$\frac{\partial P}{\partial y} = -J_x B_z \qquad (4)$$

X (axial) momentum:

$$\rho u_x \frac{\partial u_x}{\partial x} = -\frac{\partial P}{\partial x} + J_y B_z \qquad (5)$$

Energy Equation:

$$\rho \underline{u} \cdot \nabla\left(\frac{u^2}{2} + h\right) = \underline{E} \cdot \underline{J} \qquad (6)$$

Hall Effect: Calculation of the Hall current and electric field is useful in assessing this effect in the gas dynamic choking and magnetosonic choking equations. For purposes of illustration, a special case has been selected. The Hall current and field can be calculated from Ohms law for the case where the electron Hall parameter is of order 1, the ion Hall parameter is $\beta_i << 1$, and the ion slip is negligeable (s~0). These conditions are obtained when the gas is fully ionized. The electron pressure terms in Ohms law will be maintained. Electron pressure and density gradients should be significant in MPD thrusters since electrons

bear the resultant body force which accelerates the plasma. The total pressure for this isotropic case is:

$$P=P_e+P_i+P_n \tag{7}$$

Since the gas is assumed to be singly ionized, $P_n=0$, $n_e=n_i$, and $t_e=t_i$ has already been assumed, we may write:

$$P_i=P_e \tag{8}$$

and

$$\frac{\partial P_e}{\partial y} = \frac{1}{2}\frac{\partial P}{\partial y} \tag{9}$$

Using (4) in (9) allows us to write:

$$\frac{\partial P_e}{\partial y} = -\frac{1}{2} J_y B_z \tag{10}$$

Using (10) and by manipulating only the x and y components of (2) we can calculate J_x without knowledge of E_x:

$$J_x = \frac{\sigma(E_y - u_x B_z) - J_y \dfrac{(1-\beta_e^2)}{(1+\beta_e^2)}}{\dfrac{\sigma B_z}{e n_e} - \dfrac{2\beta_e}{1+\beta_e^2}} \tag{11}$$

$$E_x = \frac{1-\beta_e^2}{2\beta_e}(E_y - u_x B_z) - \frac{1}{e n_e}\frac{\partial P_e}{\partial x} + \frac{1+\beta_e^2}{2\sigma_e B_e}\left(J_y + J_x \frac{\sigma_e B_z}{e n_e}\right) \quad (12)$$

Also, we will need:

$$J_y = \left[J_x \frac{\sigma_e B_z}{2 e n_e}\frac{2\beta_e}{\sigma_e} + (1-\beta_e^2)(E_y - u_x B_z)\left(1 - \frac{1}{1 - \frac{2 e n_e}{\sigma_e B_z}}\right)\right] \cdot \left(\frac{\sigma_e}{(1+\beta_e^2)^2 - 2\beta_e}\right) \quad (13)$$

Although (11) and (12) apply for the special case of an equilibrium, fully ionized plasma, these can be used to estimate the sign and magnitude of the Hall effect. To gain some insight, simplify (11) and (12) for the case β_e=1:

$$J_x = \frac{\sigma_e (E_y - u_x B_z)}{\frac{\sigma_e B_z}{2 e n_e} - 1} \quad (14)$$

$$E_x = -\frac{1}{e n_e}\frac{\partial P_e}{\partial x} + \frac{\left(J_y + J_x \frac{\sigma_e B_z}{2 e n_e}\right)}{\sigma_e} \quad (15)$$

For σ=7500 mho/m, $0.05<B_z<0.1$, $10^{19}<n_e<10^{21}$, which are reasonable values for megawatt MPD thrusters, we find:

$$1.2 < (2en_e)/(\sigma_e B_z) < 235$$

Thus, the denominator of (14) is positive. For an accelerator, $E_y - u_x B_z$ must be positive, therefore $J_x>0$. For isothermal accelerating flow,

$$\frac{\partial n_e}{\partial x} < 0$$

hence

$$\frac{\partial P_e}{\partial x} < 0$$

therefore $E_x>0$. Evaluating the sign of E_x for more general cases is not so easily done. The product of the Hall current and field is positive, and adds energy to the flow.

Using (13) and substituting $\beta_e=1$, (14) and (15) results in:

$$J_y = \frac{\sigma_e}{1 - \frac{2e n_e}{\sigma_e B_z}} (E_y - u_x B_z) \qquad (16)$$

This can be compared to the strictly one dimensional case, equation (6) from reference 1:

$$J_y=\sigma_e(E_y - u_x B_z)$$

The Hall effect can be interpreted as increasing the conductivity by the factor

$$0 < 1-(2en_e)/(\sigma_e B_z) < 1$$

for the values cited above.

Note that (14) and (16) can be combined to eliminate $E_y-u_xB_z$:

$$J_x=J_y\, 2en_e / \sigma_e B_z \qquad (17)$$

It is now easy to calculate the Ohmic dissipation:

$$dq=(\underline{E} + \underline{u} \times \underline{B}) \qquad \text{or}$$

$$dq=(E_y-u_xB_z)J_y + +E_xJ_x$$

which can be simplified to:

$$dq= \underbrace{J_y^2 \frac{1-\frac{2en_e}{\sigma_e B_z}}{\sigma_e}}_{Y} + \underbrace{\frac{2en_e}{\sigma_e B_z}\left(2\frac{J_y^2}{\sigma_e} - \frac{J_y}{en_e}\frac{\partial P_e}{\partial x}\right)}_{X} \qquad (18a)$$

Again, comparing (18a) to the strictly one dimensional case where $dq=J_y^2/\sigma_e$, we see that Ohmic dissipation from the y field components has decreased by a factor $1-(2en_e)/(\sigma_e B_z)$, which for this example is less than one. However, dissipation from the Hall field and current more than make up for this, as seen by simplifying (18a):

$$dq= \frac{J_y^2}{\sigma_e}\left(1+\frac{2en_e}{\sigma_e B_z}\right) - \frac{J_y}{en_e}\frac{\partial P_e}{\partial x} \qquad (18b)$$

The conclusion of all this effort is that for the interesting, singly ionized case, the Hall effect increases dissipation. We can gage this effect by substituting (17) into (18b):

$$dq = \frac{J_y^2}{\sigma_e}\left(1 + \frac{J_x}{J_y}\right) - \frac{J_y}{e n_e}\frac{\partial P_e}{\partial x} \qquad (18c)$$

Experimental data of magnetic field can be mathematically transformed to current streamlines, and the ratio J_x/J_y can be visually and geometrically determined. Examination of experimental data can be used to identify regions where J_x/J_y is significant. Such areas can now be interpreted directly as incurring higher than optimal Ohmic dissipation. This basis permits direct comparison of various operating points or configurations to determine areas and conditions where Ohmic dissipation is high.

Gas Dynamic Choking: To maintain algebraic simplicity, the state equation can be written to ignore effects of density on ionization reactions. This is defensible for plasmas of a density found in MPD thrusters, according to reference[1]. The simplified equation of state is:

$$p = \rho G(h) \qquad a^2 = \frac{G}{1 - \frac{dG}{dh}} \qquad (19)$$

a = speed of sound

Combining the above equations in a manner described in reference[1], the equation for axial acceleration through Mach 1 can be written:

$$\frac{\frac{\partial u_x}{\partial x}}{J_y} = \frac{\frac{1}{J_y}\frac{G}{A}\frac{dA}{dx} - \frac{\left(1 - \frac{G}{a^2}\right)A}{\dot{m}} E_x \frac{J_x}{J_y} - \left[\frac{\left(1 - \frac{G}{a^2}\right)A}{\dot{m}} E_y - B_z\right]}{\frac{G}{u_x}\left[\frac{u_x^2}{a^2} - 1\right]} \qquad (20)$$

At the sonic singularity, (u_x=a), the numerator must also be zero, which means that the area change is zero and the electric field is specified by the relation:

$$E_x J_x/J_y + E_y = (B_z \dot{m}/A)\,(dG/dh) \tag{21}$$

This differs from ref. 1 by the addition of the Hall field E_x and current J_x. The Hall parameter is similar to J_x/J_y, and thereby affects the choking relation to first order.

Using these equations, a numerical model can be constructed that would expose the detailed behavior of gas dynamic choking and the Hall effect. The assumptions of full ionization and equilibrium state equation can be relaxed at the expense of algebraic simplicity. The development of more realistic equations still should exhibit the Hall and gas dynamic choking effects.

Magnetosonic Choking: The case where flow is fully ionized with an ideal state equation has been analyzed for a 1-D channel with area variation by Martinez[2]. The Hall effect can be assessed by using a pad of paper, (4)-(6), and eliminating all transverse derivatives in favor of axial:

$$\frac{1}{u_x}\frac{\partial u_x}{\partial x}\left\{(1-\frac{G}{a^2})\xi - 1 + \frac{G}{u_b^2}\left(\frac{u_x^2}{a^2} - 1\right)\right\}$$
$$+\frac{1}{A}\frac{\partial A}{\partial x}\left\{(1-\frac{G}{a^2})\xi - 1 - \frac{G}{u_b^2}\right\}$$
$$+\frac{1}{B_z/\rho}\frac{\partial(B_z/\rho)}{\partial x}\left\{(1-\frac{G}{a^2})\xi + 1\right\} \tag{22a}$$
$$+\left(1-\frac{G}{a^2}\right)\frac{E_x j}{\rho u_x u_b^2} = 0$$

with definitions, for convenience, of:

$$j = \frac{\sigma_e (E_y - u_x B_z)}{\frac{\sigma_e B_z}{e n_e} - \frac{2\beta_e}{1+\beta_e^2}} \tag{22b}$$

(Note: $\dot{J}$ has units of A/m^2 but is neither J_x nor J_y.)

$$u_b^2 = \frac{B_z^2}{\mu_0 \rho} \tag{22c}$$

$$\xi = \frac{E_y - E_x \delta}{u_x B_z} \tag{22d}$$

$$\delta = \frac{\frac{1-\beta_e^2}{1+\beta_e^2}}{\frac{\sigma_e B_z}{e n_e} - \frac{2\beta_e}{1+\beta_e^2}} \tag{22e}$$

Several interesting cases can be explored. First, Martinez has analyzed a case which ignores thermodynamic effects. Here this is obtained by zero temperature or taking the limit as the speed of sound approaches zero:

$$\frac{1}{u}\frac{\partial u}{\partial x}\left\{ -\xi + \frac{u^2}{u_b^2} \right\} + \frac{1}{A}\frac{\partial A}{\partial x}\left\{ -\xi \right\}$$

$$-\xi \frac{1}{B_z/\rho}\frac{\partial (B_z/\rho)}{\partial x} - \frac{E_x j}{\rho u u_b^2} = 0 \tag{23}$$

Magnetosonic choking occurs when:

$$\left(\frac{u_x}{u_b}\right)^2 = \xi \tag{24a}$$

To compare this to the Martinez approach we rewrite (24a) with (22c) and (22d):

$$\left(\frac{u_x}{u_b}\right)^2 = \frac{E_y}{u_x B_z} - \frac{E_x}{u_x B_z}\left[\frac{\frac{1-\beta e^2}{1+\beta e^2}}{\frac{\sigma_e B_z}{e n_e} - \frac{2\beta e}{1+\beta e^2}}\right] \tag{24b}$$

with the Hall parameter zero, this reduces to

$$\left(\frac{u_x}{u_b}\right)^2 = \frac{E_y - \frac{e n_e}{\sigma_e B_z}}{u_x B_z}$$

An order of magnitude estimate for (12), using typical numbers from pulsed, multimegawatt tests and $\beta_e \cong 1$, indicates E_x is of the same order as E_y. Thus for typical Hall parameters of one to ten, the right most term of (24b) indicates that magnetosonic choking is strongly affected by the Hall parameter.

SUMMARY

A buffer electrode was designed and used to prevent severe insulator erosion. Two hypotheses remain concerning the physics of it's function. Since the severe erosion was not observed in a smaller device, the effectiveness of a buffer electrode to protect the insulator in larger devices is in question. Experiments and analysis should be conducted to examine the mechanisms at work in the insulator to cathode interface.

Preliminary anode sheath analysis has been done, and should be extended to include the effects of neutral atoms and ionization. Anode heat loads can only be predicted after an accurate sheath model has been developed.

Analyses of a quasi one-dimensional approximation has illuminated the basic effect of the Hall parameter on a) Ohmic heating, b) gas dynamic, and c) magnetosonic choking effects. The approach should be useful to experimental studies in that it provides a simple way to relate magnetic field measurements, easily obtained in pulsed testing, to Ohmic dissipation.

As a result of the difficulty of solving the insulator erosion, funds were exhausted before the crucial cathode erosion measurements could be made. Future efforts in steady-state experiments should be directed at obtaining this data as the first priority.

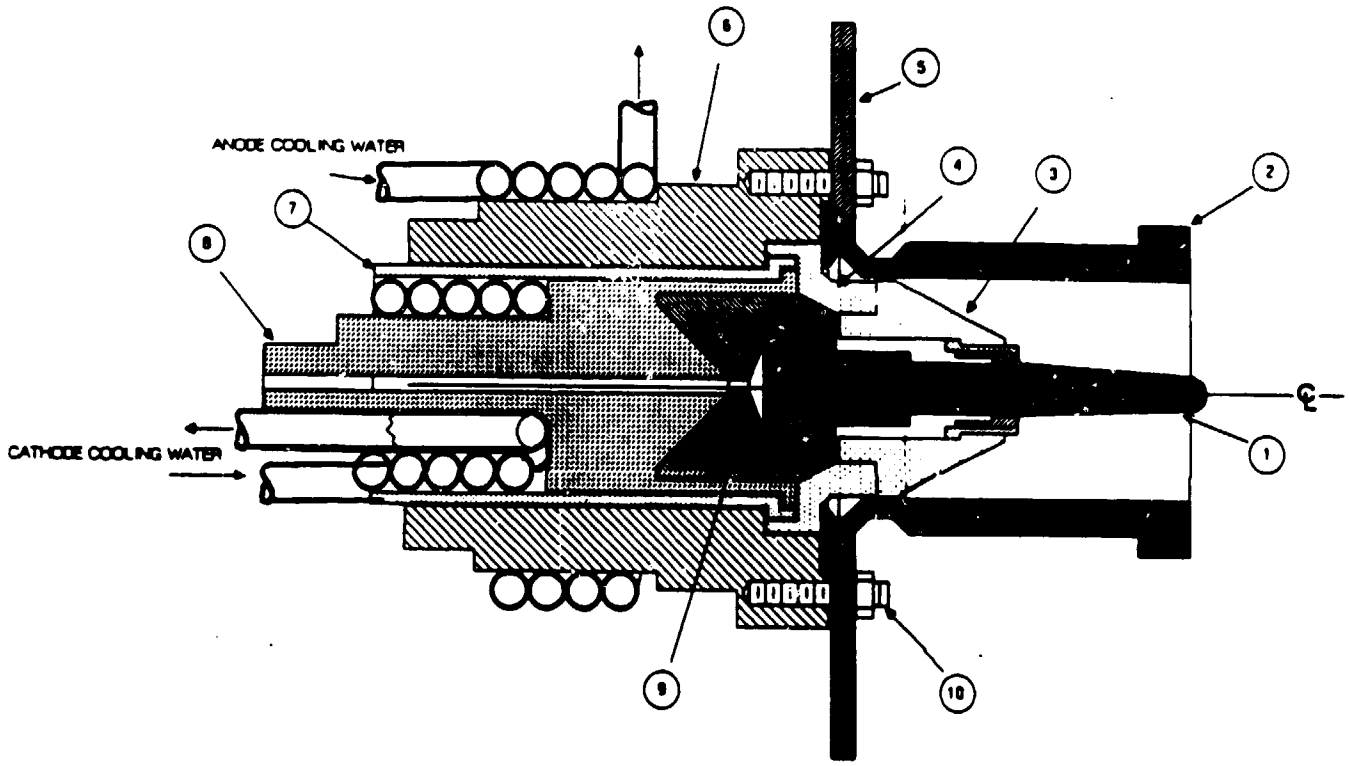

Figure 1 - 100 kW MPD Test Bed Schematic

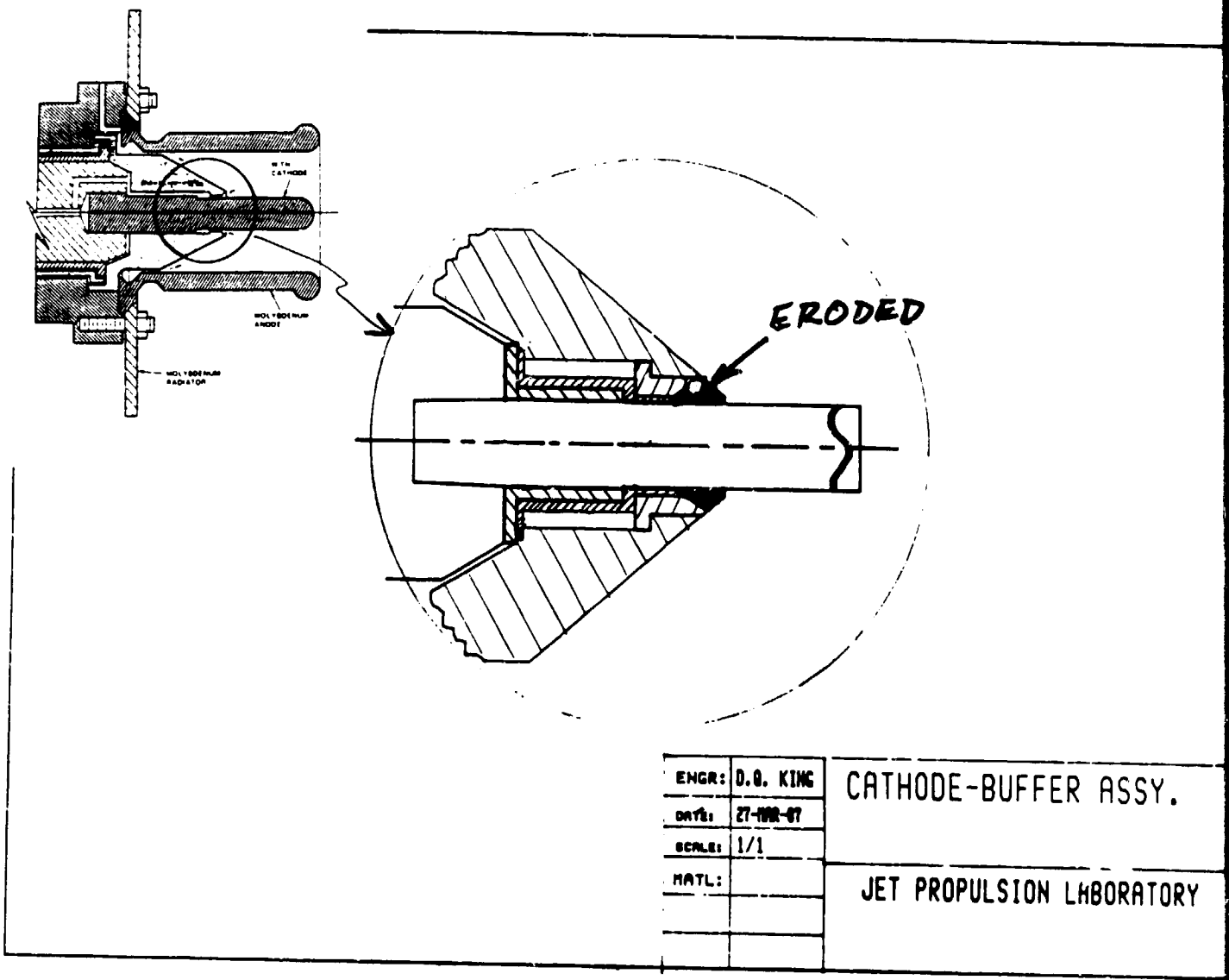

Figure 2 - Detail of Insulator Erosion

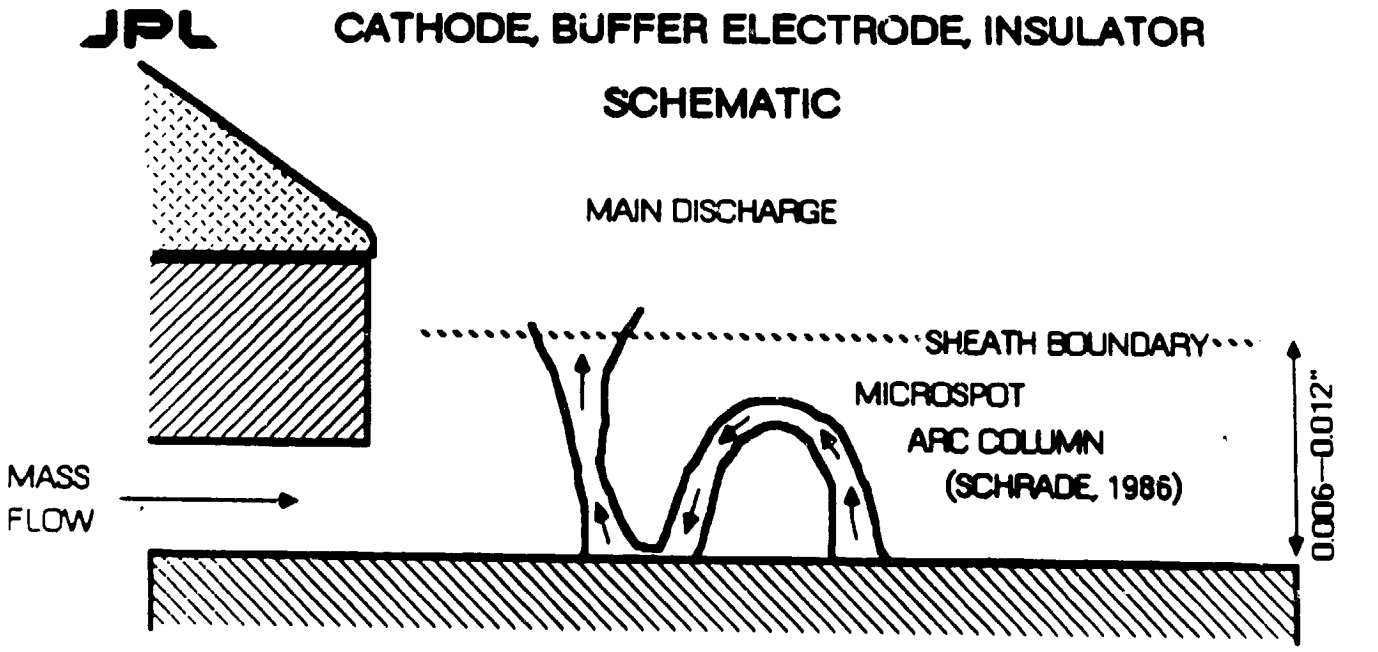

Figure 3 - Buffer Electrode Schematic

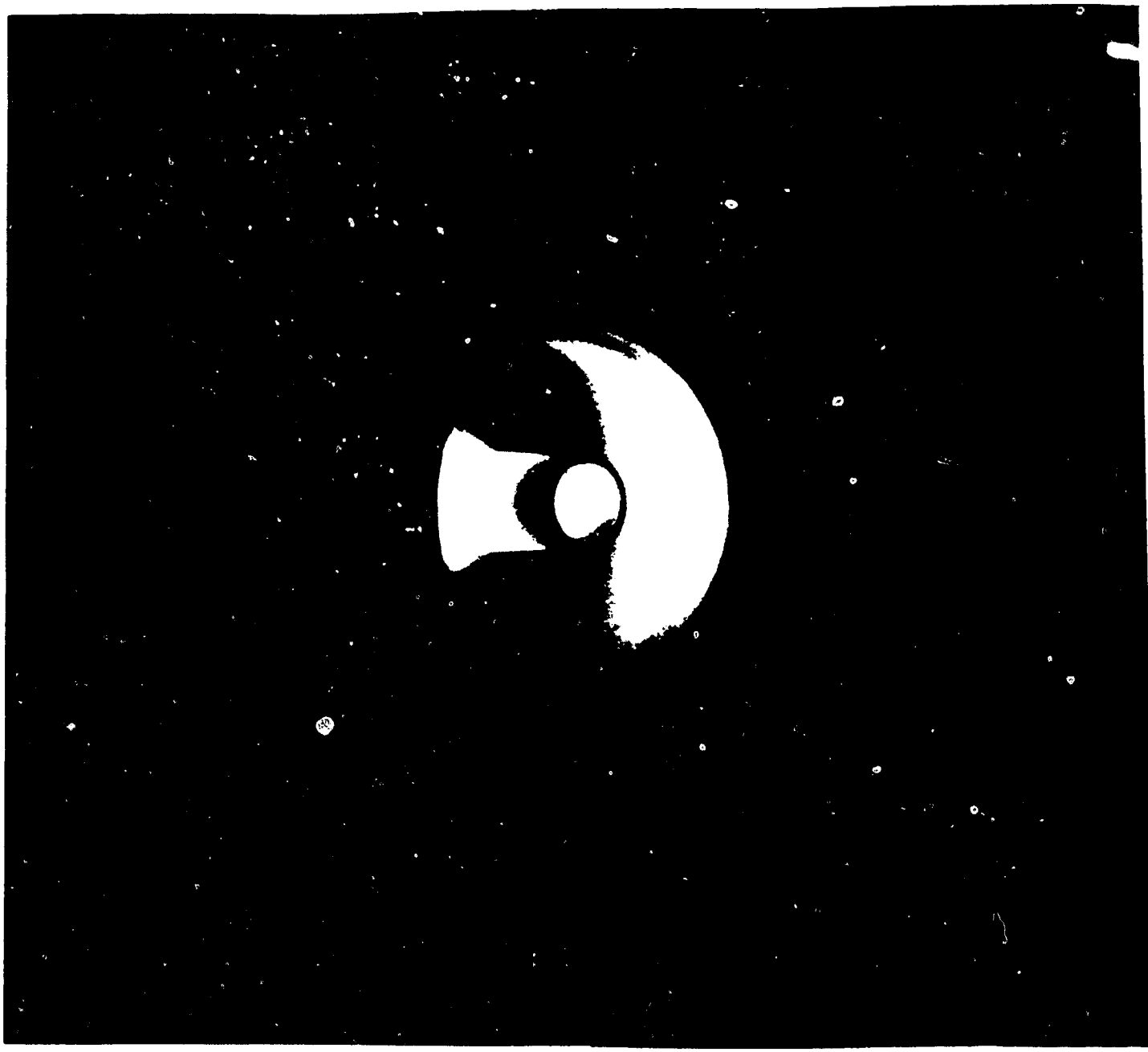

Figure 4 - Self-Field Steady-State MPD Thruster Operating at 23 kW, 0.16 g/s Argon, 1200 A, for a 83 minute run.

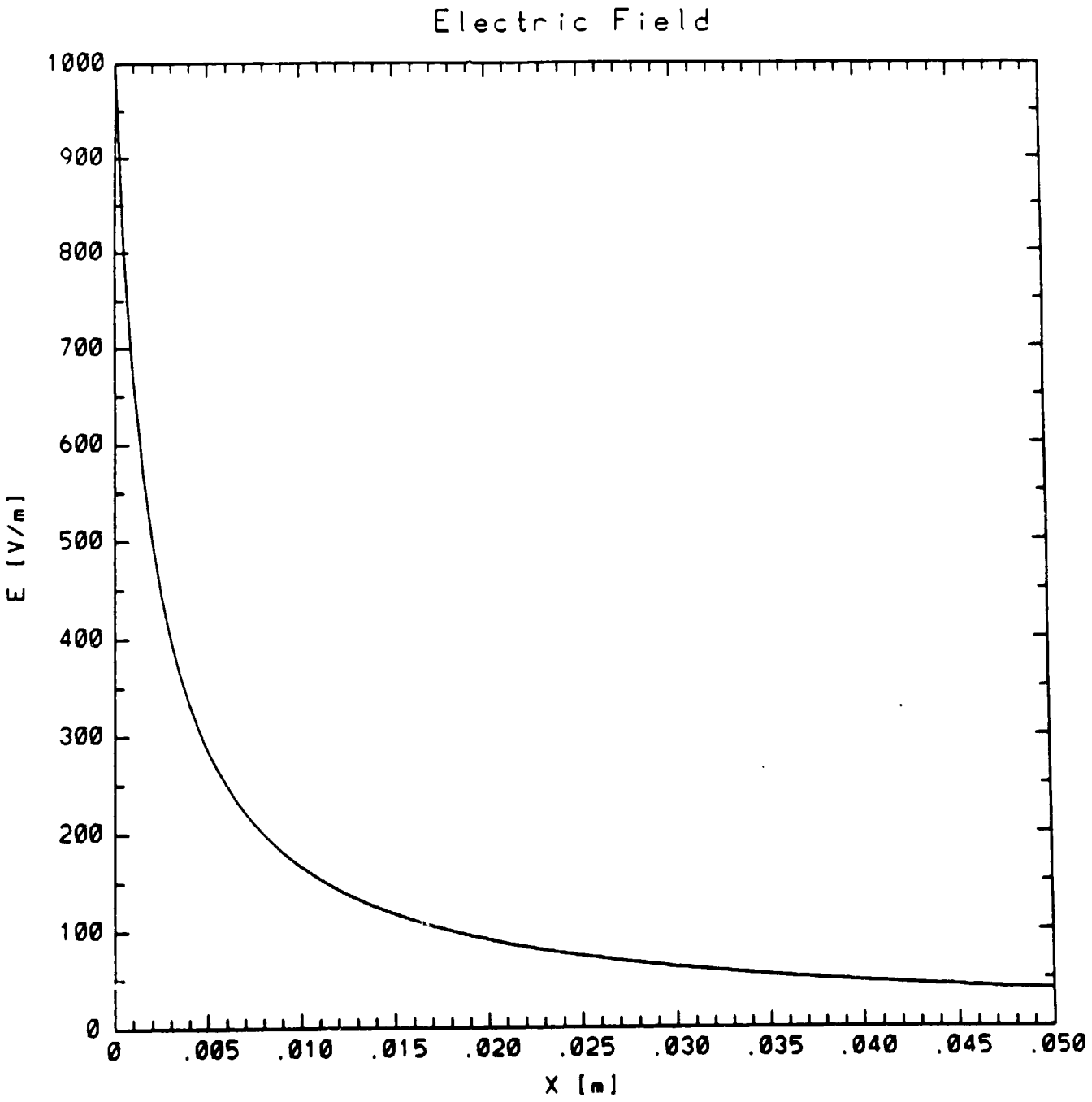

Figure 5 - Anode Sheath Electric Field vs Distance from Anode

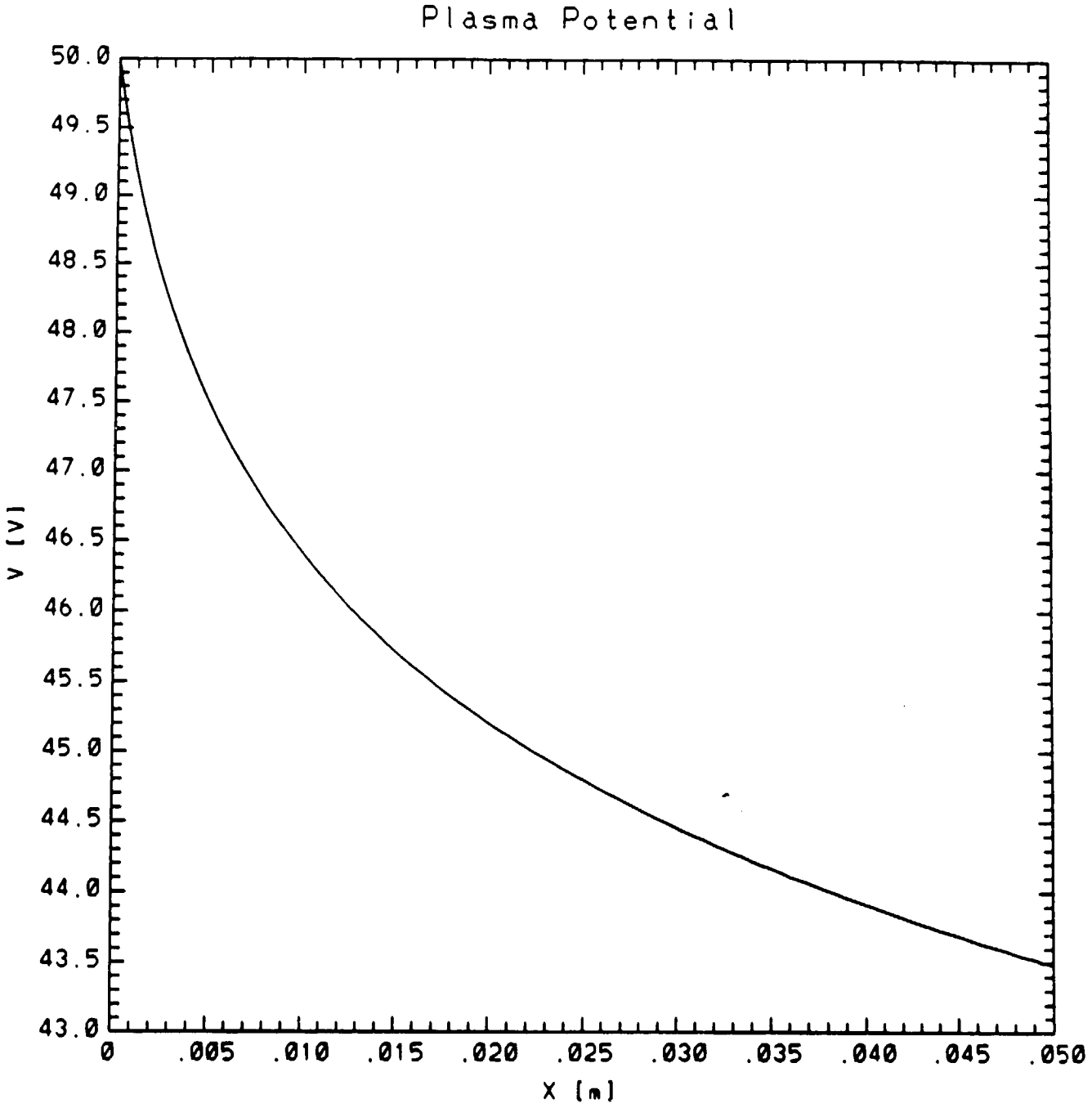

Figure 6 - Plasma Potential vs. Distance from Anode

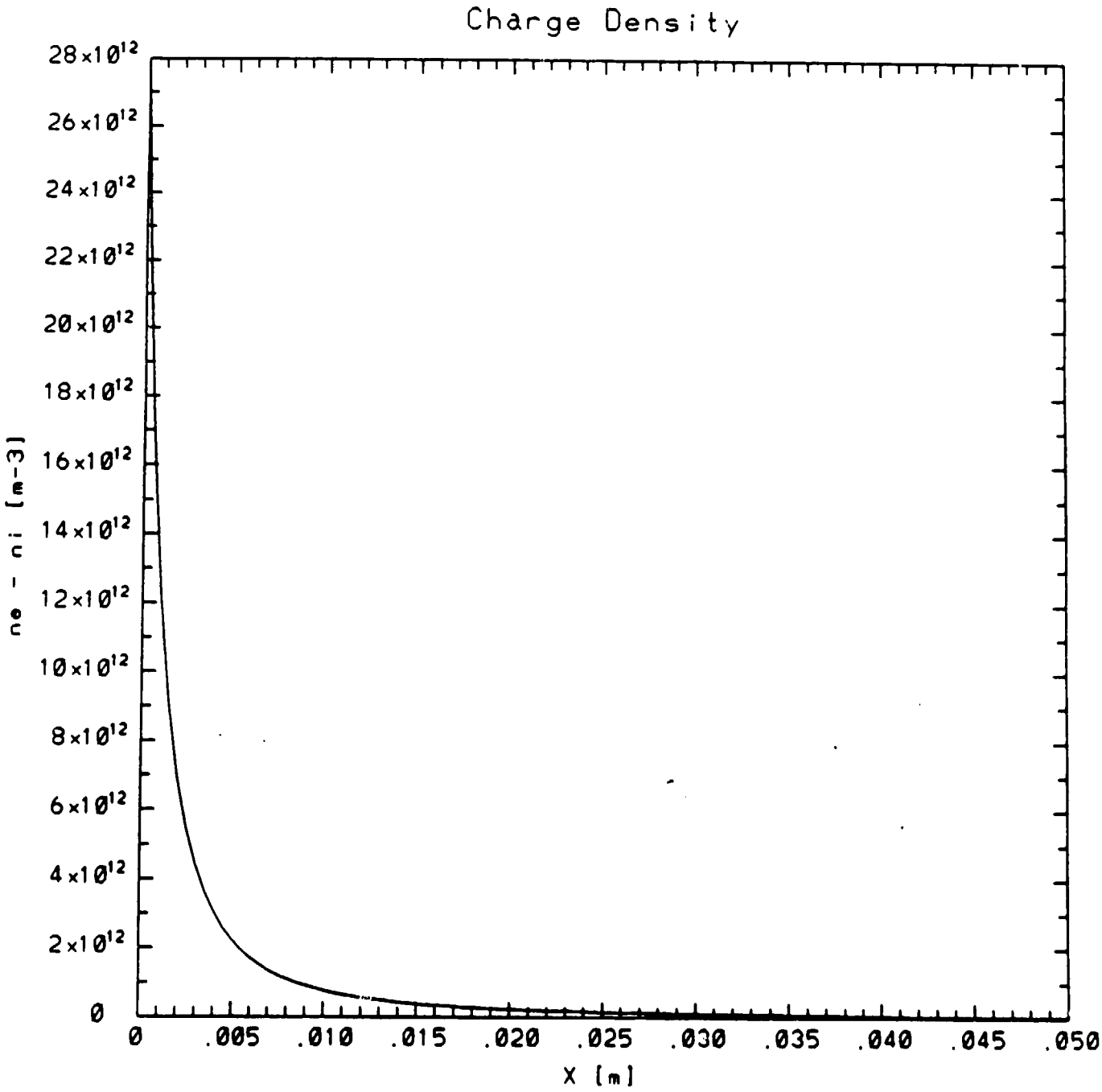

Figure 7 - Charge Density vs. Distance from Anode

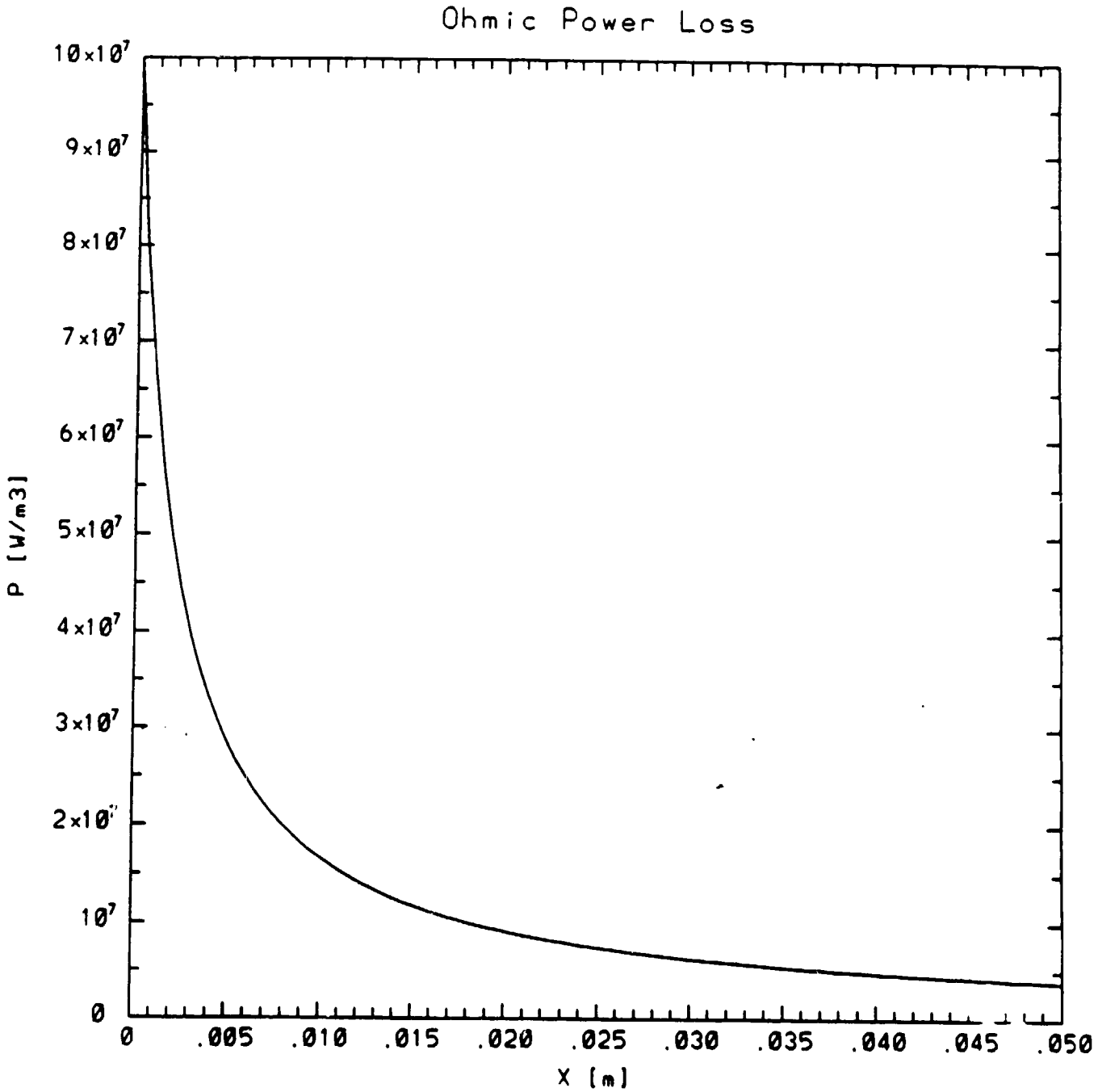

Figure 8 - Ohmic Dissipation vs. Distance from Anode

REFERENCES

1. King, D.Q., "MAGNETOPLASMADYNAMIC CHANNEL FLOW FOR DESIGN OF MPD THRUSTERS," Ph.D. Thesis, Princeton University, 1982.

2. M. Martinez-Sanchez, "Structure of Self Field Accelerated Plasma Flows," AIAA paper 87-1065.